Bioorganic & Medicinal Chemistry Letters 19 (2009) 5078–5081

Contents lists available at ScienceDirect

Bioorganic & Medicinal Chemistry Letters

journal homepage: www.elsevier.com/locate/bmcl

N-[(3*S*)-Pyrrolidin-3-yl]benzamides as novel dual serotonin and noradrenaline reuptake inhibitors: Impact of small structural modifications on P-gp recognition and CNS penetration

Florian Wakenhut [a,*], Gill A. Allan [c], Paul V. Fish [a], M. Jonathan Fray [a], Anthony C. Harrison [c], Rachel McCoy [b], Stephen C. Phillips [b], Alan Stobie [a], Dominique Westbrook [b], Simon L. Westbrook [b], Gavin A. Whitlock [a]

[a] Department of Genitourinary Chemistry, Pfizer Global Research and Development, Sandwich Laboratories, Ramsgate Road, Sandwich, Kent CT13 9NJ, UK
[b] Department of Genitourinary Biology, Pfizer Global Research and Development, Sandwich Laboratories, Ramsgate Road, Sandwich, Kent CT13 9NJ, UK
[c] Department of Pharmacokinetics, Dynamics and Metabolism, Pfizer Global Research and Development, Sandwich Laboratories, Ramsgate Road, Sandwich, Kent CT13 9NJ, UK

ARTICLE INFO

Article history:
Received 5 June 2009
Revised 3 July 2009
Accepted 7 July 2009
Available online 31 July 2009

Keywords:
N-[(3*S*)-Pyrrolidin-3-yl]benzamides
SNRI
Serotonin reuptake
Noradrenaline reuptake
CYP2D6 inhibition
P-gp recognition
MDCK-mdr1
Urinary incontinence

ABSTRACT

The structure–activity relationship and the synthesis of novel *N*-[(3*S*)-pyrrolidin-3-yl]benzamides as dual serotonin and noradrenaline monoamine reuptake inhibitors (SNRI) is described. Preferred compound **9** aka **PF-184,298** is a potent SNRI with good selectivity over dopamine reuptake inhibition (DRI), good in vitro metabolic stability, weak CYP inhibition and drug-like physicochemical properties consistent with CNS target space. Evaluation in an in vivo preclinical model of stress urinary incontinence showed **9** significantly increased urethral tone at free plasma concentrations consistent with its in vitro primary pharmacology.

Selective inhibition of serotonin (5-HT) and noradrenaline (NA) reuptake constitutes an attractive dual pharmacology approach to the treatment of a number of diseases. For example dual 5-HT/NA reuptake inhibitor duloxetine **1** has shown clinical efficacy in the treatment of depression,[1,2] diabetic neuropathic pain[3] and stress urinary incontinence (SUI).[4] For SUI, it has been reported that the prevention of urinary leakage could be mediated by stimulation of central 5-HT_2 and α_1 adrenergic receptors resulting in more effective closure of the urethral sphincter.[5] This finding reinforces the importance of identifying inhibitors exhibiting properties compatible with CNS penetration.

As part of our research efforts to identify new potential drug candidates, we have recently reported several new templates[6–11] that have delivered potent and selective SNRIs, and notably a 3-amino-pyrrolidine template that furnished compounds **2**[8] and **3**[10] (Fig. 1). Unfortunately, when compound **3** was assessed in an in vivo preclinical efficacy model for SUI[12] (Fig. 2), it did not produce statistically significant increase in Peak Urethral Pressure (PUP) at free plasma concentrations consistent with its in vitro primary pharmacology and its progression was thus halted.

We postulated that the lack of efficacy was due to poor CNS penetration as **3** was subsequently shown to have very low cerebrospinal fluid (CSF) to free plasma ratio of ~0.1 in rat and dog at steady state.[13] Our hypothesis was confirmed when the pharmacological profile of the compound was evaluated in vivo in microdialysis experiments.[14] Indeed, in these experiments, striatal 5-HT levels were markedly increased only after systemic administration of doses of compound **3** that were significantly higher than

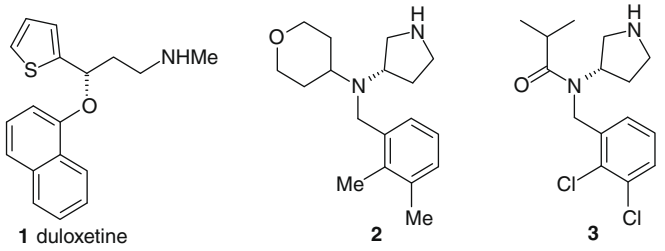

Figure 1. Structures of duloxetine and disclosed SNRIs **2** and **3**.

* Corresponding author. Tel.: +44 1304 640950; fax: +44 1304 651987.
E-mail address: florian.wakenhut@pfizer.com (F. Wakenhut).

0960-894X/$ - see front matter © 2009 Elsevier Ltd. All rights reserved.
doi:10.1016/j.bmcl.2009.07.049

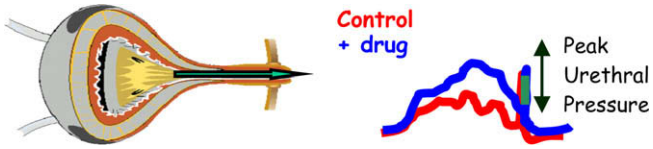

Figure 2. Schematic of urethral tone model.[12] A pressure transducer is introduced in the urethra, up to the bladder neck then taken out slowly whilst recording the pressure. The difference in PUP between control and drug expressed as a percentage is the direct efficacy measure.

expected based on the data observed after intrastriatal perfusion of compound **3**. As **3** exhibited physicochemical properties consistent with CNS target space[15] (m. wt. 315; clog *P* 3.3; log $D_{7.4}$ 0.8; pK_a 9.4; HBD 1; HBA 3; TPSA 32 Å^2) we further hypothesised that the poor CNS penetration was probably the result of recognition by the P-glycoprotein transporter (P-gp). Indeed, a significant degree of efflux was observed when **3** was assessed in the MDCK-mdr1 cell line (15/64 ER = 4.3).[16]

In order to reduce the level of P-gp recognition we elected to disrupt the H-bonding capability of the molecule as it has been demonstrated to be a key factor for recognition.[17] As preliminary structure activity relationship (SAR) investigations had already established that the pyrrolidine secondary amine was key to potency, we decided to focus our attention on the amide group. Our main strategy was to isomerize the amide into the benzylic position hoping that in doing so we would disrupt P-gp recognition. This modification led to the discovery of a novel series of *N*-[(3*S*)-pyrrolidin-3-yl]benzamide derivatives (Fig. 3). The SAR of these amides **7**–**30** is discussed in this Letter. Furthermore the ADME, safety and efficacy profile of compound **9** aka **PF-184,298** is also reported.

Target test compounds were conveniently prepared from commercially available homochiral *N*-BOC-3-amino pyrrolidine **4** by the general methods described in Scheme 1. Secondary amines **5** were prepared either by (i) standard reductive amination under hydride or hydrogenolysis conditions of amine **4** with the appropriate aldehydes or ketones, or (ii) coupling of amine **4** with the appropriate activated acid followed by reduction of the corresponding amide with borane–THF complex, or (iii) palladium catalysed N-arylation of amine **4** with bromobenzene. Amines **5** were subsequently converted into amides **6** by benzoylation with the appropriate benzoyl chloride. Finally HCl or TFA deprotection of the *N*-BOC amines provided required targets **7**–**30**. It is worth noting that this synthetic route was highly amenable to parallel synthesis therefore facilitating SAR exploration.

Initial SAR investigations focused on the variation of the R^1 group with the benzamide substitution R maintained as 2,3-di-Cl (Table 1). A series of analogues **7**–**14** were prepared with alkyls of increasing size. Interestingly, with the exception of the ethyl substituent, probably too small (compound **7**), all groups at R^1 were accommodated, affording several potent and balanced SNRIs (ratios of activities SRI:NRI, 1:1 to 1:4). We were also pleased to

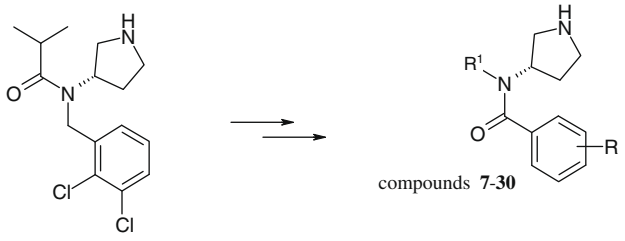

Figure 3. Structure of new *N*-[(3*S*)-pyrrolidin-3-yl]benzamides **7**–**30**.

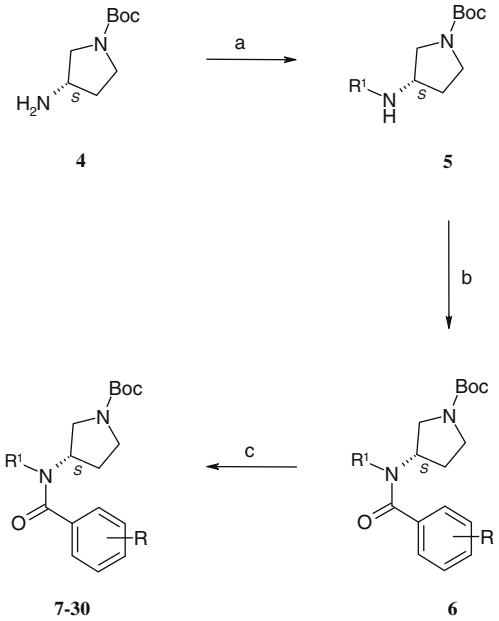

Scheme 1. Reagents and conditions: (a) (i) aldehyde/ketone, MeOH–PhMe, rt, then $NaBH_4$, MeOH, rt or aldehyde/ketone, H_2 (60 psi), 10% Pd-C, EtOH, rt; (ii) R′COCl, NEt_3, CH_2Cl_2, rt or R′CO_2H, 1-propanephosphonic acid (T3P), NEt_3, CH_2Cl_2, rt then BH_3·THF, THF, reflux; (iii) tris(dibenzylideneacetone)dipalladium(0) (5 mol %), 1,1′-binaphthalene-2,2′-diylbis-(diphenyl)phosphine (10 mol %), PhBr, PhMe, 100 °C; (b) ArCOCl, NEt_3, CH_2Cl_2 or dioxane rt; (c) TFA, CH_2Cl_2, rt or 4 N HCl in dioxane, rt.

find that selectivity over DRI, metabolic stability and selectivity over ion channel activity (K^+, hERG) consistent with our project objectives could be achieved as illustrated by compounds **9** and **13**. Increasing polarity, for example by introduction of a branched 4-tetrahydropyranyl (compound **15**), or replacing the alkyl substituent by a phenyl (compound **16**) was also tolerated providing additional potent and balanced SNRIs. From this analysis the isobutyl group was selected as the R^1 group and a broader set of R substituents with different substitution patterns was investigated (compounds **17**–**29**). This analysis demonstrated that (i) 2,3-disubstitution was generally the preferred substitution pattern for dual activity as can be seen when comparing compound **9** with compounds **17**–**20**; (ii) replacing one or both of the chlorine atoms with other substituents generally resulted in an erosion in NRI activity as illustrated by compounds **21** to **27**; (iii) the series could also deliver selective inhibitors of the serotonin transporter (SRI) as illustrated by compound **28** with a single 2-Cl, 4-F substituent or selective inhibitors of the noradrenaline transporter (NRI), for example compound **29** with a single 2-iPr substituent. Finally, it is also worth noting that although the (*R*)-enantiomer possessed SRI activity its NRI potency was inferior to the (*S*) (**13** vs **30**, SRI:NRI 1:13).

From these experiments, a small set of compounds emerged as preferred, exhibiting potent SNRI activity in combination with good selectivity over DRI and were selected for further profiling in the MDCK-mdr1 cell line (Table 2).

We were very pleased to find that our strategy of disrupting P-gp recognition had been successful, as compound **9** exhibited good membrane permeability combined with a reduced efflux ratio compared to **3** (ER = 2.7 vs 4.3). However not all benzamide derivatives demonstrated reduced efflux ratios and small structural modifications did result in significant differences. This is well illustrated when comparing **9** and **13**. Indeed, despite having similar physicochemical properties these compounds exhibited different efflux ratios (2.7 for **9** and 6.4 for **13**). Finally, the worst compound in this assay was **15** as it demonstrated poorer membrane permeability,

Table 1
In vitro inhibition of human monoamine reuptake[a,b], metabolic stability, K^+ hERG channel activity, clog *P* for compounds **7–30**[c]

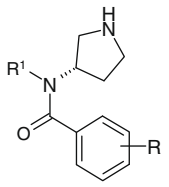

7-29

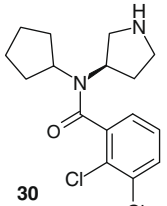

30

Compound	R	R^1	5-HT K_i (nM)	NA K_i (nM)	DA K_i (nM)	HLM Cl_{int} (μl/min/mg)	K^+, hERG IC_{50} (nM)	clog *P*
Duloxetine	—	—	5	45	435			4.3
3	—	—	9	52	640	<7.6	24,700	3.4
7	2,3-Di-Cl	Ethyl	29	217	1090	<13	>20,000	2.6
8	2,3-Di-Cl	*n*-Propyl	16	36	630	<7	>18,600	3.2
9	2,3-Di-Cl	*i*-Butyl	6	21	544	11	20,000	3.6
10	2,3-Di-Cl	CH_2CF_3	39	95	3730	<8	>10,000	2.9
11	2,3-Di-Cl	CH_2CH_2c-Propyl	15	24	404	26	7140	3.7
12	2,3-Di-Cl	CH_2t-Butyl	4	13	273	NT	16,800	4
13	2,3-Di-Cl	*c*-Pentyl	6	11	983	<7	10,300	3.6
14	2,3-Di-Cl	$CH(Ethyl)_2$	20	37	2600	34	7740	4
15	2,3-Di-Cl	4-Tetrahydropyranyl	6	10	945	13	>40,000	1.8
16	2,3-Di-Cl	Phenyl	3	11	501	<25	7920	3.7
17	2,4-Di-Cl	*i*-Butyl	3	37	2400	26	NT	3.7
18	2,5-Di-Cl	*i*-Butyl	54	198	2430	29	19,800	3.7
19	3,5-Di-Cl	*i*-Butyl	6	43	3070	NT	>10,000	3.7
20	3,4-Di-Cl	*i*-Butyl	4	50	430	36	17,200	3.7
21	3-Cl	*i*-Butyl	19	135	1330	23.5	NT	3
22	2-Cl, 3-CF_3	i-Butyl	11	103	2070	NT	4120	3.7
23	2-Me,3-Cl	*i*-Butyl	3	29	516	26	52,400	3.5
24	2-Me,3-F	*i*-Butyl	13	69	1610	21	NT	2.9
25	2-Cl, 3-F	*i*-Butyl	15	67	2370	20	NT	3.1
26	2-F, 3-Cl	*i*-Butyl	10	139	2560	26	>10,000	3.1
27	2-CF_3, 3-F	*i*-Butyl	25	26	NT	NT	>10,000	3.4
28	2-Cl, 4-F	*i*-Butyl	7	263	2540	20	NT	3.1
29	2-*i*-Propyl	*i*-Butyl	1320	65	3590	<7	12,900	3.6
30	2,3-Di-Cl	*c*-Pentyl	13	169	3090	NT	NT	3.6

[a] See Ref. 9 and 11 for definitions of terms and complete details of assay conditions.
[b] Monoamine reuptake K_i are geometric means of a minimum of 2 experiments. Differences of <2-fold should not be considered significant.
[c] NT denotes not tested.

Table 2
Profile of compounds **3**, **9**, **13** and **15** in the MDCK-mdr1 cell line

	MDCK-mdr1 AB/BA $P_{app} \times 10^{-6}$ cm s^{-1}	MDCK-mdr1, ER
3	15/64 ($n = 2$)	4.3
9	16/43 ($n = 3$)	2.7
13	10/64 ($n = 3$)	6.4
15	1/20 ($n = 1$)	20

probably as a result of its lower lipophilicity and extra oxygen atom, in combination with an increased efflux ratio ER = 20.

Compound **9** was selected for further evaluation based on the combination of its superior profile in the MDCK-mdr1 cell line, metabolic stability in human liver microsomes (HLM) predictive of low in vivo clearance, and selectivity over ion channel activity consistent with our project objectives as measured by binding to the hERG channel. (Table 3).

Additional screening in in vitro ADME screens showed **9** to have excellent metabolic stability in human hepatocytes. Compound **9** also exhibited weak inhibition of all major CYP450 enzymes (2D6, 3A4, 1A2, 2C9, 2C19, IC_{50}s >30 μM) and good membrane permeability in the CaCO-2 cell line, therefore predicting for good oral absorption. Finally, when compound **9** was evaluated for broader pharmacological activity in a panel of receptors, ion channels and enzymes (Cerep, BIOPRINT™), it was found to be highly selective exhibiting binding affinity (>50% inhibition at 10 μM) only for the Na channel (site 2; IC_{50} = 3.6 μM), the sigma receptor (IC_{50} = 5.1 μM) and the kappa opioid receptor (IC_{50} = 5.8 μM).

Table 3
Physicochemical properties, ADME profiles and K^+ channel affinities of compound **9**[a]

	9
MW	315
clog *P*/log $D_{7.4}$	3.6/0.6
HBD/HBA count	1/3
pK_a	10
TPSA, Å^2	32
HLM, Cl_i μL/min/mg	11
h.heps, Cl_i μL/min/millions cells	3
CYP2D6 inh. (dextromethorphan), IC_{50} (nM)	>30,000
CYP1A2 inh. (tacrine), IC_{50} (nM)	>30,000
CYP2C9 inh. (diclofenac), IC_{50} (nM)	>30,000
CYP2C19 inh. (S-methphenytoin), IC_{50} (nM)	>30,000
CYP3A4 inh. (felodipine), IC_{50} (nM)	>30,000
CYP3A4 inh. (midazolam), IC_{50} (nM)	>30,000
CYP3A4 inh. (testosterone), IC_{50} (nM)	>30,000
CaCO-2, AB/BA @10 μM, $P_{app} \times 10^{-6}$ cm s^{-1}	12/26
K^+, hERG, K_i (nM)	20,000

[a] See Ref. 9 for definitions of terms and assays.

To demonstrate the impact of the reduced P-gp recognition on blood brain barrier (BBB) penetration, the CSF to unbound plasma concentration ratio was measured in the rat following a steady state infusion regimen. We were pleased to find that the observed ratio of 0.45 was superior to the ratio of 0.1 observed for compound **3.** Now confident that **9** had significantly improved CNS penetration compared to **3**, its performance was evaluated in the anaesthetized dog model described above (Fig. 4).[12] From this

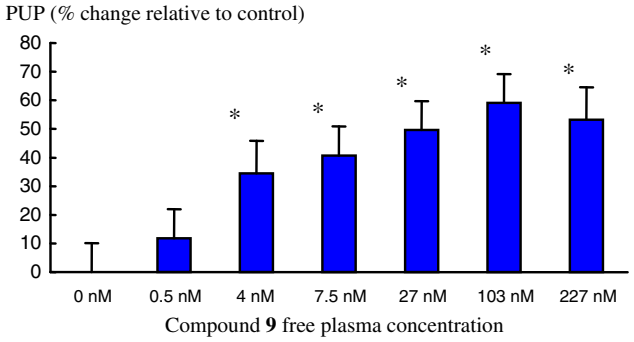

Figure 4. The effects of compound **9** on peak urethral pressure expressed as percentage change relative to control. Data is expressed as the mean ± SEM and significant difference relative to control is denoted thus * $p < 0.05$ ($n = 4$, n denotes the number individual animals used to generate a cumulative dose response via iv infusion of compound to a steady state free plasma concentration. Each bar represents the mean response versus mean free plasma concentration for each step). Dog functional potency for compound **9** was dSRI $IC_{50} = 7.4$ nM (platelet, $n = 18$), dNRI $IC_{50} = 28.6$ nM (carotid artery, $n = 15$).[19]

study, it is evident that **9** significantly increases urethral tone in a dose dependent manner. Furthermore, at an unbound plasma concentration of 4 nM, **9** increases PUP in the dog by 35%. To put this result into context, this is superior to the 26% increase induced in this model by 4.5 nM duloxetine, a concentration we estimate to be close to human therapeutic free plasma concentrations based on published human pharmacokinetic data[18] and in-house human plasma protein binding determinations (estimated free C_{max} 5–10 nM at 40 mg *bid*).

Finally, **9** was found to be clean in a package of in vitro and in vivo genetic toxicology screens, produced no dose-limiting toxicity in acute and sub-chronic (14-day) oral rat and dog toxicology screens and did not exhibit significant effect on spontaneous locomotor activity vs vehicle control in rats when administered orally up to 15 mg/kg.

In summary, we have described the discovery of novel benzamide derivatives as potent SNRIs. More specifically, compound **9** aka **PF-184,298** exhibited potent SNRI activity in combination with good DRI selectivity, good metabolic stability, weak CYP inhibition, low affinity for ion channels and no significant off-target pharmacology. Furthermore, isomerisation of the amide moiety to the benzylic position resulted in a significant reduction in P-gp recognition that translated into improved BBB penetration. When **PF-184,298** was assessed in a dog in vivo preclinical model for stress urinary incontinence, it elicited a dose dependent increase in PUP superior to that observed with SNRI duloxetine. Finally, **PF-184,298** did not produce dose-limiting toxicity in preclinical toxicology screens and was progressed to human clinical studies. The results of these studies will be reported in future publications.

Acknowledgements

We wish to thank Carol Bains, Gerwyn Bish, Timothy Buxton, Edelweiss Evrard, Arnaud Lemaitre, Debbie Lovering, Edward Pegden, Bhairavi Patel, and Melanie Skerten for compound synthesis. We are also grateful to Caroline Tolley and Doreen Davey for screening data, Katherine Fenner and Ian Gurrell for generating the MDCK-mdr1 data and to Kelly Conlon for providing the urethral tone model materials and methods summary.

Supplementary data

Supplementary data associated with this article can be found, in the online version, at doi:10.1016/j.bmcl.2009.07.049.

References and notes

1. (a) Jann, M. W.; Slade, J. H. *Pharmacotherapy* **2007**, *11*, 1571; (b) Montgomery, S. *Int. J. Psych. Clin. Pract.* **2006**, *10*, 5; (c) Jackson, S. *Curr. Med. Res. Opin.* **2005**, *21*, 1669.
2. (a) Wernicke, J. F.; Iyengar, S.; Ferrer-Garcia, M. D. *Curr. Drug Ther.* **2007**, *2*, 161; (b) Bauer, M.; Moeller, H.-J.; Schneider, E. *Exp. Opin. Pharmacotherapy* **2006**, *7*, 421.
3. Kajdasz, D. K.; Iyengar, S.; Desaiah, D. *Clin. Ther.* **2007**, *29*, 2536.
4. (a) Mariappan, P.; Alhasso, A.; Ballantyne, Z.; Grant, A.; N'Dow, J. *Eur. Urol.* **2007**, *51*, 67; (b) Steers, W. D.; Herschorn, S.; Kreder, K. J.; Moore, K.; Strohbehn, K.; Yalcin, I.; Bump, R. C. *BJU Int.* **2007**, *100*, 337.
5. Thor, K. B.; Kirby, M.; Viktrup, L. *Int. J. Clin. Pract.* **2007**, *61*, 1349.
6. (a) Fray, M. J.; Bish, G.; Brown, A. D.; Fish, P. V.; Stobie, A.; Wakenhut, F.; Whitlock, G. A. *Bioorg. Med. Chem. Lett.* **2006**, *16*, 4345; (b) Fray, M. J.; Bish, G.; Fish, P. V.; Stobie, A.; Wakenhut, F.; Whitlock, G. A. *Bioorg. Med. Chem. Lett.* **2006**, *16*, 4349.
7. Fish, P. V.; Fray, M. J.; Stobie, A.; Wakenhut, F.; Whitlock, G. A. *Bioorg. Med. Chem. Lett.* **2007**, *17*, 2022.
8. Whitlock, G. A.; Blagg, J.; Fish, P. V. *Bioorg. Med. Chem. Lett.* **2008**, *18*, 596.
9. Fish, P. V.; Deur, C.; Gan, X.; Greene, K.; Hoople, D.; Mackenny, M.; Para, K. S.; Reeves, K.; Ryckmans, T.; Stiff, C.; Stobie, A.; Wakenhut, F.; Whitlock, G. A. *Bioorg. Med. Chem. Lett.* **2008**, *18*, 2562.
10. Wakenhut, F.; Fish, P. V.; Fray, M. J.; Gurrell, I.; Mills, J. E.; Stobie, A.; Whitlock, G. A. *Bioorg. Med. Chem. Lett.* **2008**, *18*, 4308.
11. SNRI activity of target compounds was established using scintillation proximity assay (SPA) technology by assessing their ability to inhibit binding of selective radioligands at the human 5-HT, NA and DA transporters. Cellular membrane preparations generated from recombinant HEK293 cells expressing a single monoamine transporter were utilised for these experiments. For details of the assay conditions, see: Andrews, M. D.; Brown, A. D.; Fish, P. V.; Fray, M. J.; Lansdell, M. I.; Ryckmans, T.; Stobie, A.; Wakenhut, F.; Gray, D. L. F. WO Patent 064351, 2006, pp 56–59. The BioByte software was used to assess clog *P*.
12. Adult, female, nulliparous beagle dogs were anaesthetised initially with sodium pentobarbitone to induce surgical anaesthesia (30 mg/kg iv), and then transferred to α-chloralose anaesthetic (70–100 mg/kg iv induction followed by constant infusion to deliver 10–15 mg/kg/h iv for the duration of the experiment), following completion of surgery. Animals were intubated, and respiration maintained at a constant rate of 14 breaths per minute. Tidal volume was adjusted to maintain expired air within normal physiological limits. Throughout the experiment the animal was maintained at a core body temperature of approximately 37 °C using a thermocouple heated blanket (Harvard Apparatus Ltd., Kent, UK). Cannulation of superficial vessels was carried out to allow administration of compounds, blood sampling, infusion of anaesthetic, and monitoring of arterial pressure (Millar, 7F, Millar Instruments, US). A midline incision was made in the abdomen to expose the bladder. The ureters were cannulated to drain urine throughout the experiment. The dome of the bladder was cannulated and the cannula fed through the bladder to the external urethra. This catheter was used to introduce the urethral pressure catheter (Millar SUPC-380C), into the urethra. The bladder was filled with saline to achieve an intravesical pressure of approximately 8–10 mmHg, and bladder pressure was measured by connecting the bladder catheter to a pressure transducer (Model DTX plus, Becton-Dickenson UK Ltd, Oxford, UK). Following completion of surgery, animals were allowed to stabilise for at least 60 minutes before starting urethral pressure profilometry measurements. Urethral pressure profilometry (UPP) was measured by withdrawing the pressure transducer through the urethra at a constant rate. A full profile measurement was obtained approximately every 6 min, and readings were taken continuously throughout the experiment. Baseline measurements were performed until 4 consistent measurements were identified, after which drug administration commenced. From the profilometry data, peak urethral pressure was measured (PUP, mmHg). Changes in PUP were compared with mean baseline value and expressed as % change from baseline, recorded over the 4 consecutive profiles obtained prior to test drug or vehicle administration. All experiments involving animals were carried out in compliance with national legislation, specifically the UK Animal (Scientific Procedures) Act 1986, and subject to local ethical review.
13. Measuring CSF levels is commonly used as a way to assess Blood Brain Barrier penetration, see: (a) Lin, L. H. *Curr. Drug. Metab.* **2008**, *9*, 46; (b) Feng, M. R. *Curr. Drug. Metab.* **2002**, *3*, 647.
14. Deecher, D. C.; Beyer, C. E.; Johnston, G.; Bray, J.; Shah, S.; Abou-Gharbia, M.; Andree, T. H. *J. Pharm. Exp. Ther.* **2006**, *318*, 657.
15. Mahar Doan, K. M.; Humphreys, J. E.; Webster, L. O.; Wring, S. A.; Shampine, L. J.; Serabjit-Singh, C. J.; Adkison, K. K.; Polli, J. W. *J. Pharm. Exp. Ther.* **2002**, *303*, 1029.
16. The MDCK-mdr1 cell line is commonly used to assess P-gp recognition, see: Hammarlund-Udenaes, M.; Bredberg, U.; Friden, M. *Curr. Top. Med. Chem.* **2009**, *9*, 148.
17. For a substrate model of the P-gp transporter, see: Seelig, A. *Eur. J. Biochem.* **1998**, *251*, 252.
18. (a) Chan, C.; Yeo, K. P.; Pan, A. X.; Lim, M.; Knadler, M. P.; Small, D. S. *Br J. Clin. Pharm.* **2006**, *63*, 310; (b) kinner, M. H.; Kuan, H.; Pan, A.; Sathirakul, K.; Knadler, M. P.; Gonzales, C. R.; Yeo, K. P.; Reddy, S.; Lim, M.; Ayan-Oshodi, M.; Wise, S. D. *Clin. Pharm. Ther.* **2003**, *73*, 170.
19. For detailed experimental procedures see Supplementary data.